Vitreous Humor Proteomic Profile in Patients With Vitreoretinal Lymphoma

Hiroyuki Komatsu,[1] Yoshihiko Usui,[1] Kinya Tsubota,[1] Risa Fujii,[2] Takefumi Yamaguchi,[3] Kazuichi Maruyama,[4] Ryo Wakita,[1] Masaki Asakage,[1] Kazuki Hamada,[1] Naoyuki Yamakawa,[1] Naoya Nezu,[1] Koji Ueda,[2] and Hiroshi Goto[1]

[1]Department of Ophthalmology, Tokyo Medical University, Tokyo, Japan
[2]Cancer Proteomics Group, Cancer Precision Medicine Center, Japanese Foundation for Cancer Research, Tokyo, Japan
[3]Department of Ophthalmology, Tokyo Dental College Ichikawa General Hospital, Chiba, Japan
[4]Department of Ophthalmology, Osaka University Graduate School of Medicine, Osaka, Japan

Correspondence: Yoshihiko Usui, Department of Ophthalmology, Tokyo Medical University Hospital, 6-7-1 Nishi-Shinjuku, Shinjuku-ku, Tokyo 160-0023, Japan; usuyoshi@gmail.com.

Received: June 29, 2023
Accepted: November 10, 2023
Published: December 1, 2023

Citation: Komatsu H, Usui Y, Tsubota K, et al. Vitreous humor proteomic profile in patients with vitreoretinal lymphoma. *Invest Ophthalmol Vis Sci.* 2023;64(15):2. https://doi.org/10.1167/iovs.64.15.2

Purpose. Vitreoretinal lymphoma is a high-grade malignant non-Hodgkin lymphoma with poor prognosis. The objective of this study was to elucidate the proteome profile of the vitreous in patients with vitreoretinal lymphoma (VRL), aiming to advance understanding of the pathophysiology of VRL.

Methods. Comprehensive proteomic analyses of vitreous humor using liquid chromatography with tandem mass spectrometry were performed for 10 patients with VRL, 10 control patients with idiopathic epiretinal membrane or macular hole, and 10 patients with ocular sarcoidosis. Differentially expressed proteins (DEPs) were identified by comparing VRL with controls and sarcoidosis, and functional pathway analysis was performed. Finally, vitreous concentrations of representative DEPs that were significantly upregulated in proteomics study were measured by ELISA using a separate cohort.

Results. In total, 1594 proteins were identified in the vitreous humor of VRL, control, and sarcoidosis samples. Also, 282 DEPs were detected in VRL, 249 upregulated and 33 downregulated, compared with controls. Enrichment pathway analysis showed alterations in proteasome-related pathways. Compared to controls and sarcoidosis, 14 DEPs in VRL showed significant upregulation. In the validation study, ELISA confirmed significantly higher vitreous concentrations of PSAT1, YWHAG, and 20S/26S proteasome complex in VRL compared with controls and sarcoidosis. Among the upregulated DEPs, vitreous PITHD1 and NCSTN concentrations correlated positively with vitreous IL-10 concentrations.

Conclusions. This study highlights aberrations in protein expression pattern in the vitreous of patients with VRL. The DEPs identified in this study may play pivotal roles in VRL pathogenesis, providing insights to enhance understanding of VRL pathophysiology and contribute to the development of VRL biomarkers.

Keywords: vitreoretinal lymphoma, proteomics, ubiquitination, uveitis, pathogenesis

Vitreoretinal lymphoma (VRL) is a high-grade malignant non-Hodgkin lymphoma and a subtype of primary central nervous system lymphoma (PCNSL), typically classified as diffuse large B-cell lymphoma (DLBCL).[1,2] In an epidemiological study on uveitis conducted at a university hospital in Japan in 2016, VRL accounted for 2.6% of all uveitis cases.[3] Furthermore, VRL has a poor prognosis, with 5-year survival rate of 61%, according to a nationwide survey in Japan,[4] and median overall survival of 12 to 35 months in the United States.[5] Delayed diagnosis of VRL is common due to the similarities it shares with other uveitis conditions. When ocular lesions are the initial manifestation, central nervous system (CNS) infiltration that directly impacts the prognosis occurs frequently, occurring in approximately 56% to 90% of the cases within a few years of onset.[4,6] On the other hand, cases of primary CNS lymphoma infiltrating the eye represent approximately 10% to 20% of VRL. Additionally, reports indicate that 16% to 34% of cases presenting with ocular lesions at the onset of VRL already have CNS lesions.[2] The frequency of involvement of primary organs other than CNS, known as secondary (metastatic) cases, is approximately 12.4%.[7] Therefore, early diagnosis of VRL is of great importance for deciding appropriate work-up and treatment strategies and improving prognosis.

However, VRL remains a masquerade syndrome and is frequently misdiagnosed as chronic idiopathic uveitis due to its indistinct clinical manifestations and absence of conclusive biomarkers.[8,9] Cytology, polymerase chain reaction (PCR) analysis of the monoclonality of immunoglobulin H (IgH), and measurement of interleukin (IL)-10 and IL-6 levels are considered the gold standard diagnostic tests for VRL. In a Japanese survey, cytology demonstrated a modest

detection rate of 44.5%.[4] Similarly, the detection rates of PCR analysis for IgH receptor rearrangements were also limited, with 80% in VRL cases presenting vitreous opacity and 75% in VRL cases with subretinal infiltration. IL-10 serves as a better diagnostic biomarker for VRL, with a detection rate of 90% in cases manifesting vitreous opacity and subretinal infiltration. However, it should be noted that an elevated IL-10 level in the vitreous is not sufficient to diagnose intraocular or CNS lymphoma. For example, approximately 10% to 20% of VRL cases have shown IL-10 to IL-6 ratios below 1.[4] Further clarification of the underlying molecular mechanisms and discovery of diagnostic biomarkers are imperative.

The promise of an omics approach to decipher the pathogenesis of various complex diseases has been well documented. Our group has previously proposed potential biomarkers for VRL using omics resources such as microRNA,[10] and has demonstrated the presence of unique microRNA signatures in patients with VRL. Proteomics, a significant component in the field of omics, has also surfaced as a promising tool for the discovery of biomarkers due to its ability to quantify large numbers of proteins in a single experiment, offering valuable insights into the pathophysiology of diseases. In the field of ophthalmology, proteomics has been used to investigate various ocular tissues including aqueous humor, retina, and vitreous,[11–14] as well as to study DLBCL, throughout the last decade.[15–18] To the best of our knowledge, vitreous proteomic profiling of VRL has not been reported. The present study aimed to elucidate the vitreous proteomic profile to inform the pathophysiology of VRL and explore the potential use for identification of new diagnostic biomarkers and therapeutic targets.

Materials and Methods

Patients

Sixty patients were included in this study, including 20 patients with VRL, 20 disease controls, and 20 patients with ocular sarcoidosis diagnosed at Tokyo Medical University Hospital from 2017 to 2019. Patients with VRL who had not been treated with corticosteroids within 1 month before vitrectomy were enrolled. Excluded from the study were patients with preoperative trauma, vitreous hemorrhage, pre-existing macular pathologies including age-related macular degeneration, and immunodeficiency. VRL was diagnosed according to current diagnostic criteria based on clinical characteristics, radiographic examination, blood tests, vitreous cytopathological examination, molecular genetic (such as gene rearrangement) analyses, and ratios of IL-6 to IL-10 in intraocular fluid, as described previously.[1,4,19–22] Patients in the control group consisted of 10 patients with epiretinal membrane and 10 with macular hole who underwent vitreous surgery for treatment. Patients with ocular sarcoidosis, which is an inflammatory disease and a type of granulomatous uveitis, were analyzed and compared with patients with VRL, aiming to further identify the alterations in VRL-specific proteins.

A comprehensive proteome analysis was conducted in 10 cases each of VRL, control, and ocular sarcoidosis. Clinical information is described in Supplementary Table S1. Subsequently, vitreous concentrations of selected proteins were measured by ELISA using a separate validation cohort also consisting of 10 cases each of VRL, control, and ocular sarcoidosis, distinct from the ones used in the initial proteome analysis. Table 1 summarizes the demographic and clinical data of the three groups in the proteomics cohort and the validation cohort.

This study was conducted in accordance with the tenets of the Declaration of Helsinki. The study was approved by the institutional review board of Tokyo Medical University (approval number: SH3281), and written informed consent was provided by all patients.

Sample Collection and Preprocessing

Vitreous samples used in this study were collected when the patients underwent diagnostic or therapeutic vitrectomy. One vitreous humor sample from each patient was used for analysis. Vitreous humor samples (approximately 0.5 to 1.0 mL per sample) were harvested from the mid-vitreous region at the commencement of a standard three-port 25-gauge vitrectomy and were removed with a vitreous cutter prior to intraocular infusion. The samples were immediately sent to a cytology and molecular laboratory (SRL, Inc., Tokyo, Japan) for VRL diagnostic tests. After centrifugation at 3000*g* for 3 minutes, the supernatants were collected and preserved at –80°C for molecular analyses. Cell pellets were used for cytology examination.

Comprehensive Proteomic Analyses

We conducted comprehensive proteomic profiling using the vitreous humor samples in the proteomics cohort comprised of 10 patients with VRL compared with 10 disease controls and 10 patients with ocular sarcoidosis. Proteomic analysis was conducted using liquid chromatography with tandem mass spectrometry (LC-MS/MS). Then, to study alterations of VRL-specific protein expression, we conducted bioinformatic analysis on the proteins identified by LC-MS/MS compared with ocular sarcoidosis. The proteomics data of VRL, ocular sarcoidosis, and controls in this study are deposited in ProteomeXchange (PXD046153) and in the jPOST database[23] (JPST002347).

Mass Spectrometric Analysis

Sample processing for proteome analysis was conducted as per previous reports.[14,24] Briefly, vitreous samples were digested with Trypsin/Lys-C Mix (V5073; Promega, Madison, WI, USA). The peptides were then analyzed using an UltiMate 3000 RSLCnano UHPLC System (Thermo Fisher Scientific, Waltham, MA, USA) equipped with a 0.075-mm × 250-mm AURORA column (IonOpticks, Melbourne, Australia) in conjunction with an Orbitrap Fusion Lumos Tribid Mass Spectrometer (Thermo Fisher Scientific). Proteins from the LC-MS/MS datasets were identified by searching the SwissProt Human Database using the Mascot (Matrix Science, London, UK) or Sequest HT (Thermo Fisher Scientific) search engine. Finally, the Proteome Discoverer 2.4 software (Thermo Fisher Science) facilitated protein identification and quantification.

Bioinformatic Analysis

To elucidate protein expression alterations in VRL, proteins identified by LC-MS/MS were analyzed by multiple methodologies including Venn diagram, volcano plot,

Investigative Ophthalmology & Visual Science

Table 1. Demographic and IL Data for Patients With VRL, Epiretinal Membrane or Macular Hole (Controls), or Ocular Sarcoidosis in the Cohorts for Comprehensive Proteomics Analysis and Validation

	VRL	Controls	Ocular Sarcoidosis
Proteomics cohort			
Cases, *n*	10	10	10
Age (y), mean ± SD	63.4 ± 11.1	62.1 ± 13.3	69.5 ± 10.1
Sex, *n*			
Male	2	5	2
Female	8	5	8
IL-10 (pg/mL), mean ± SD	2199 ± 2740	—	6.22 ± 6.20*
IL-6 (pg/mL), mean ± SD	70.14 ± 77.3	—	420 ± 477*
IL-10:IL-6 ratio, mean ± SD	35.1 ± 38.7	—	0.05 ± 0.07*
Validation cohort			
Cases, *n*	10	10	10
Age (y), mean ± SD	70.5 ± 11.1	65.9 ± 7.3	59.7 ± 13.3
Sex, *n*			
Male	6	5	4
Female	4	5	6
IL-10 (pg/mL), mean ± SD	2938 ± 3468	—	6.02 ± 4.91*
IL-6 (pg/mL), mean ± SD	49.05 ± 31.4	—	76.7 ± 67.6*
IL-10:IL-6 ratio, mean ± SD	49.1 ± 45.2	—	0.23 ± 0.26*

* IL-10 and IL-6 in ocular sarcoidosis were available from only six cases in both the proteomics cohort and validation cohort.

and heatmap. Venn diagrams were created using BioRender (https://www.biorender.com/), and Prism 9 (GraphPad Software, San Diego, CA, USA) was used to generate and analyze volcano plots. Heatmaps were produced and visually presented using Morpheus (https://software.broadinstitute.org/morpheus/). Enrichment pathway analysis was performed using Reactome[25] (https://reactome.org/) and KEGG pathway with ShineyGO 0.77[26] (http://bioinformatics.sdstate.edu/go/). Finally, protein–protein interaction networks were visualized using Metascape[27] (https://metascape.org/).

Validation of Differential Protein Expression by ELISA

To validate whether differential protein expression patterns revealed by proteomic analysis using LC-MS/MS are reflected by differences in vitreous protein concentrations, we measured the concentrations of selected candidate biomarker proteins in vitreous humor samples by ELISA in a separate cohort. The candidate biomarker proteins assayed were PSAT1, YWHAG, and 20S/26S proteasome complex, using the following kits: phosphoserine aminotransferase 1 (PSAT1) ELISA Kit (Cloud-Clone Corp., Katy, TX, USA), human 14-3-3 protein gamma (YWHAG) ELISA Kit (Cusabio, Houston, TX, USA), and 20S/26S Proteasome ELISA kit (Enzo Life Sciences, Farmingdale, NY, USA) according to the manufacturers' instructions.

Statistical Analysis

All statistical analyses were performed using SPSS Statistics (IBM, Chicago, IL, USA) and R 4.3.0 (R Foundation for Statistical Computing, Vienna, Austria). Proteins with concentrations below the limit of detection were assigned a value of one-half the detection limit. A P value less than 0.05 was considered significant. Data of protein concentrations are expressed as mean ± SD. Comparisons of expressed proteins between diseases were performed using Student's t-test and adjusted using the false discovery rate (FDR) by the Benjamini–Hochberg method.[28] Correlation was assessed using Pearson's correlation coefficient. In the validation study using ELISA, because the data were not normally distributed, the results are expressed in median with interquartile range. Mann–Whitney U test was used in statistical analysis.

Results

Vitreous Proteomic Profile in VRL Compared With Controls

A total of 1594 proteins were identified in all the vitreous samples from VRL, control, and patients with ocular sarcoidosis using high-throughput proteomic analysis. Among the 1594 vitreous proteins, 1571 were detected in VRL, 1425 in ocular sarcoidosis, and 1163 in control patients (Fig. 1A). Of these proteins, 1138 were common proteins found in all three groups, but 150 were detected only in patients with VRL.

In the next step, to identify differentially expressed proteins (DEPs) in VRL, proteins with FDR-adjusted P values less than 0.05 and $\log_2$ fold changes >1 were extracted as proteins with differential expression compared with controls and ocular sarcoidosis. In this analysis, 282 proteins were detected as DEPs in VRL compared with controls, including 249 upregulated and 33 downregulated proteins; 17 proteins were detected as DEPs in VRL compared with ocular sarcoidosis, including 16 upregulated and one downregulated proteins (Figs. 1B, 1C; Supplementary Table S2). The results indicated a significant deviation in vitreous proteomic profile in VRL compared with controls, with markedly elevated expression of numerous proteins possibly associated with tumor cell metabolism in VRL, including PSAT1 associated with serine biosynthesis and HMGB2 associated with mitochondrial energy metabolism. The same feature of almost exclusively upregulated DEPs in VRL was also observed even when compared with ocular sarcoidosis, a granulomatous uveitis.

As a subsequent step, we conducted enrichment pathway analysis to identify the functional role of the DEPs in

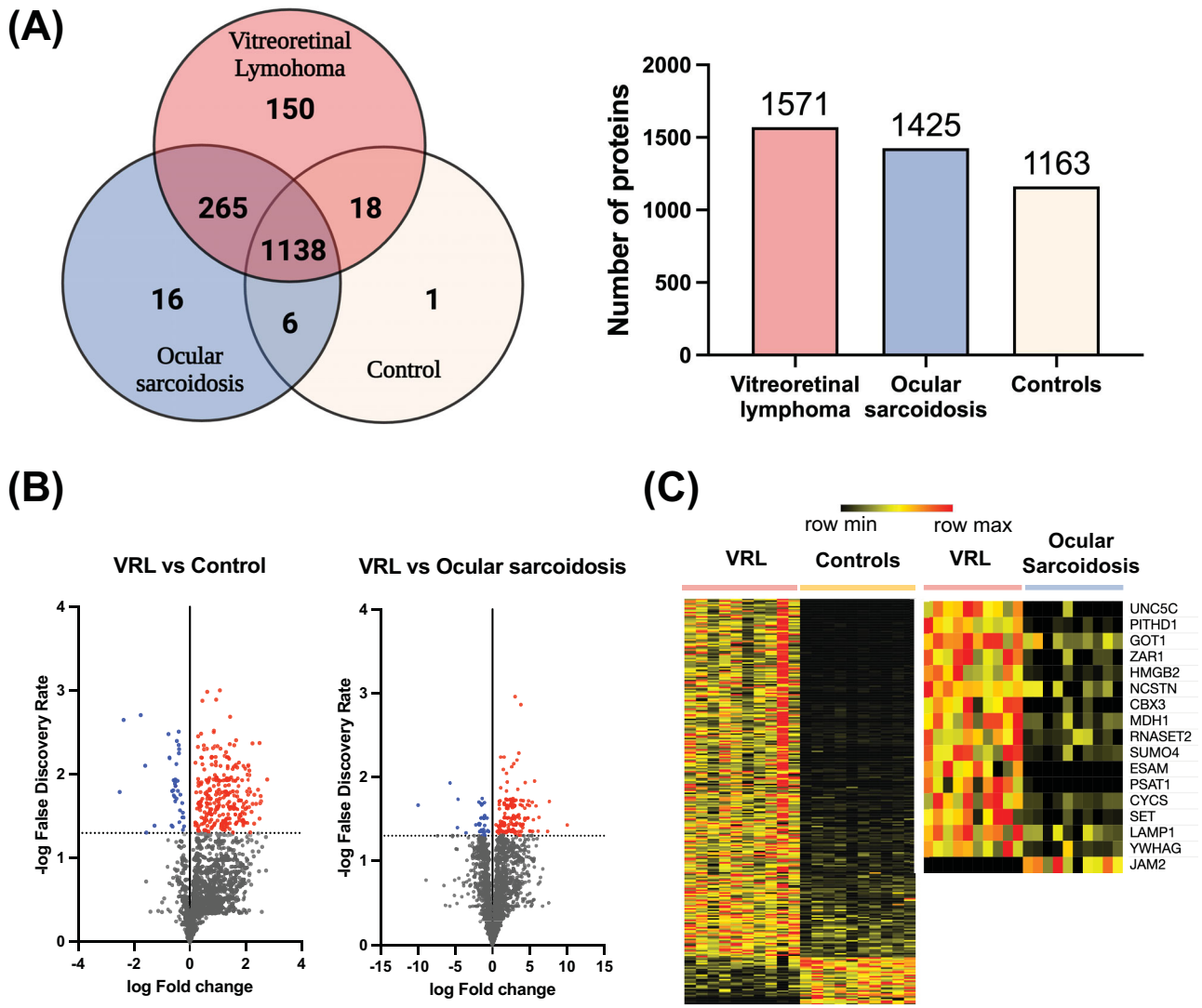

Figure 1. Identification of differentially expressed proteins in VRL compared with controls and ocular sarcoidosis. (**A**) A total of 1594 proteins were detected; among these, 1138 were common proteins expressed in VRL, control, and ocular sarcoidosis samples. The number of proteins detected in the vitreous was 1571 for VRL, 1425 for ocular sarcoidosis, and 1163 for controls, with the largest number in VRL. (**B**) The volcano plots display 282 DEPs that include 249 upregulated (*red*) and 33 downregulated (*blue*) in VRL versus controls, and 17 DEPs that include 16 upregulated and one downregulated in VRL versus ocular sarcoidosis. (**C**) The heatmaps of differentially expressed proteins in VRL clearly demonstrate distinct expression patterns separating VRL from controls and from ocular sarcoidosis.

VRL protein alteration. A search using the Reactome and KEGG pathways identified alterations in various pathways associated with the DEPs in VRL compared with controls. As shown in the top 20 pathways in Fig. 2 and Supplementary Table S2, in the KEGG pathway, "proteasome" was the most altered followed by metabolic pathways including "2-oxocarboxylic acid metabolism" and "the citrate cycle (TCA cycle)." In the Reactome pathway, "nuclear events mediated by NFE2L2" was the most significantly altered. In the top 20 Reactome pathways, the main pathway "cell cycle" was the most frequently altered. Cell proliferation-associated pathways such as "programmed cell death" and "cellular responses to stimuli" were also altered, suggesting their potential involvement in tumor cell proliferation. Of note, 10 proteins (PSMA7, PSMB6, PSMA5, PSMA6, PSMB4, PSMA3, PSMB5, PSMA4, PSMB2, and PSMA2) were associated with the most significantly altered pathways in both Reactome and KEGG pathways. These proteins are components of the 20S proteasome. Moreover, these 20S proteasome proteins were associated with all of the top 20 Reactome pathways that were altered (listed in Supplementary Table S3), implicating their significant role in pathway alteration observed in VRL.

We finally examined the protein–protein interaction (PPI) network of DEPs in VRL using Metascape. The Molecular Complex Detection (MCODE) algorithm was employed to pinpoint densely connected network components. PPI enrichment analysis based on MCODE for the DEPs in VRL revealed 11 PPI modules (Fig. 3, Supplementary Table S4). Among these 11 PPI modules, MCODE4 containing a cluster of proteasome-related proteins was identified as having the highest score. The score reflects the connectivity of each node within the network, as determined by MCODE. From these results, proteins composing the 20S proteasome may reflect the local molecular pathogenesis in the vitreous of patients with VRL.

Investigative Ophthalmology & Visual Science

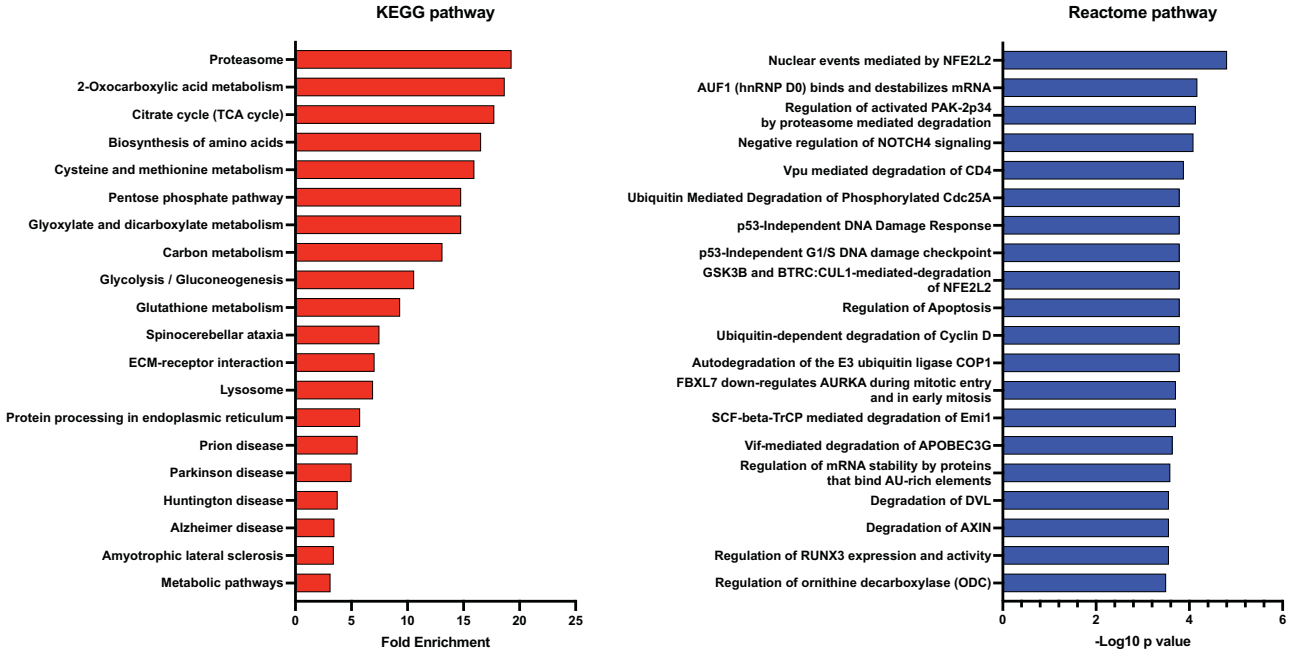

Figure 2. Top 20 altered KEGG and Reactome pathways identified by enrichment pathway analysis of DEPs in the vitreous of patients with VRL. Proteins in the most altered pathways including "proteasome" in the KEGG pathway and "nuclear events mediated by NFE2L2" in the REACTOME pathway contain the 20S proteasome protein.

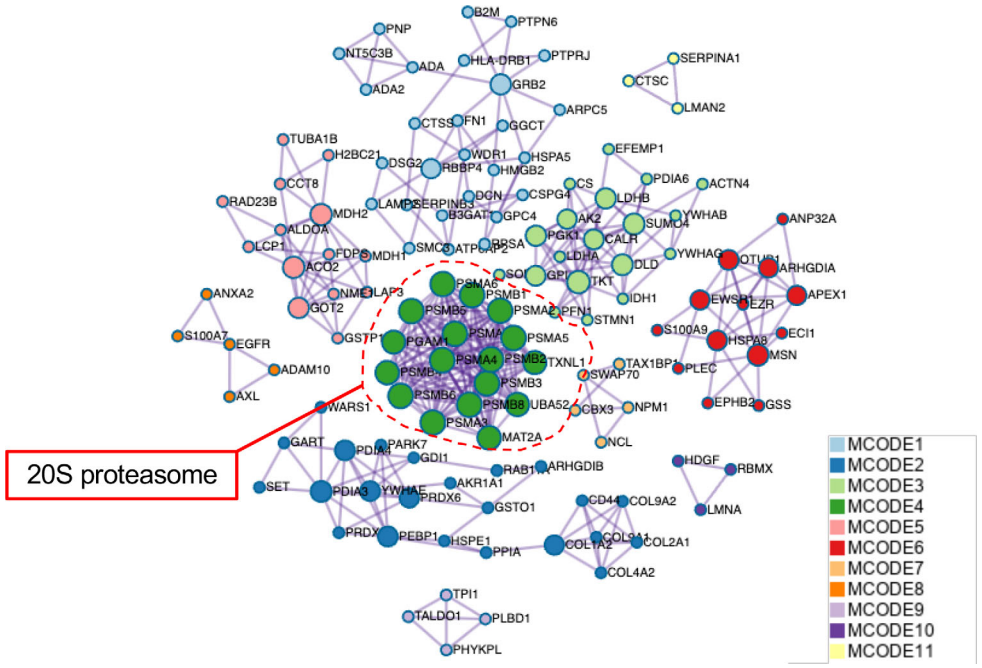

Figure 3. PPI network of differentially expressed proteins in vitreoretinal lymphoma. The MCODE algorithm depicts 11 PPI modules. The MCODE4 module composed of proteasome-related proteins is identified as the cluster with the highest score.

Detection of Specific Candidate Biomarker Proteins

Given that DEPs may partially reflect non-specific changes due to inflammatory responses, we compared the vitreous proteomic profile between VRL and ocular sarcoidosis, an inflammatory disease, in an attempt to discriminate protein alterations specific to VRL. We searched the 282 DEPs compared with controls and the 17 DEPs compared with ocular sarcoidosis to find common DEPs showing significant alterations in expression level. Fourteen proteins were identified, and their expression levels were elevated compared to both the control group and the ocular sarcoidosis group (Table 2). The 14 proteins identified as upregulated

Table 2. Differentially Expressed Proteins Upregulated in Vitreous of VRL Compared With Both Controls and Ocular Sarcoidosis

		Versus Controls			Versus Ocular Sarcoidosis		
Abbreviation	Protein Name	Log_2 FC	Adjusted *P*	Expression Status	Log_2 FC	Adjusted *P*	Expression Status
PSAT1	Phosphoserine aminotransferase 1	6.34	0.00075	Upregulation	5.627	0.0356	Upregulation
PITHD1	PITH domain-containing 1	3.58	0.00102	Upregulation	3.805	0.0044	Upregulation
CBX3	Chromobox 3	5.29	0.00075	Upregulation	3.543	0.0166	Upregulation
SET	SET nuclear proto-oncogene	6.94	0.00107	Upregulation	3.391	0.0446	Upregulation
HMGB2	High mobility group box	8.30	0.00117	Upregulation	3.298	0.02	Upregulation
UNC5C	Unc-5 netrin receptor C	3.13	0.00107	Upregulation	3.028	0.0035	Upregulation
ZAR1	Zygote arrest 1	5.51	0.00075	Upregulation	2.855	0.0221	Upregulation
SUMO4	Small ubiquitin-like modifier 4	7.44	0.00075	Upregulation	2.588	0.0241	Upregulation
CYCS	Cytochrome C, somatic	2.58	0.00022	Upregulation	1.975	0.0367	Upregulation
MDH1	Malate dehydrogenase 1	2.98	0.00022	Upregulation	1.888	0.0288	Upregulation
YWHAG	14-3-3 Protein gamma	4.75	0.00022	Upregulation	1.879	0.0468	Upregulation
NCSTN	Nicastrin	2.06	0.00022	Upregulation	1.559	0.0185	Upregulation
RNASET2	Ribonuclease T2	1.44	0.00072	Upregulation	1.474	0.0259	Upregulation
LAMP1	Lysosomal-associated membrane protein 1	1.36	0.00072	Upregulation	1.111	0.0427	Upregulation

FC, fold change.

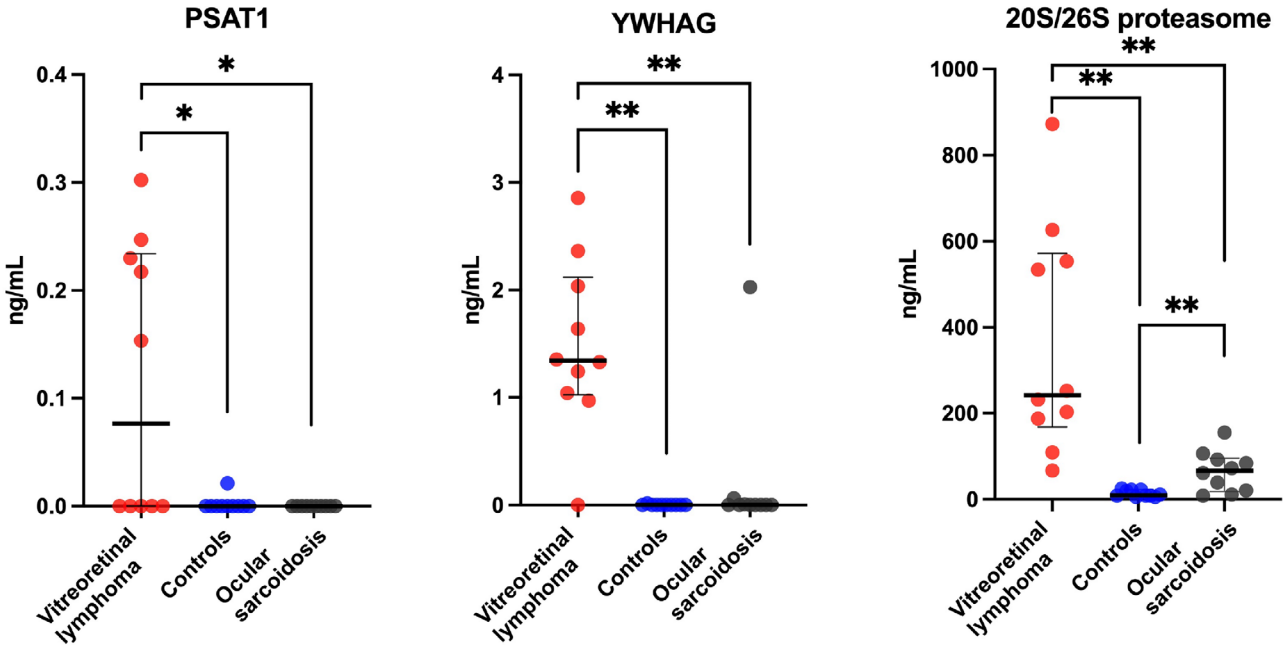

Figure 4. Vitreous concentrations of candidate VRL-specific proteins measured by ELISA in a validation cohort. Group data are expressed as median (*horizontal bar*) with interquartile range (*vertical bar*). Vitreous PSAT1 and YWHAG concentrations are significantly higher in VRL compared to controls and ocular sarcoidosis. Vitreous concentration of the 20S/26S proteasome complex is also significantly elevated in VRL compared to both ocular sarcoidosis and controls. *$P < 0.05$ and **$P < 0.01$ by Mann–Whitney *U* test.

in VRL included those involved in cellular metabolism, such as PSAT1 (related to serine metabolism) and PITHD1 (associated with cellular processes). Additionally, transcription-related proteins such as CBX3, SET, and HMGB2 were also upregulated. Of note, SUMO4 and YWHAG were significantly upregulated proteins involved in ubiquitination, closely related to the proteasome pathway that was found to be altered in the pathway analysis.

Next, we validated whether the differential protein expressions in vitreous measured quantitatively by LC-MS/MS are reflected in differences in vitreous protein concentrations measured by ELISA using a validation cohort. As candidate marker proteins, we selected PSAT and YWHAG that were highly upregulated in proteomics study. In addition, because pathway analysis indicated a significant relationship of proteasomes with VRL, we also selected the 20S/26S proteasome complex (Fig. 4). The concentrations of PSAT1 measured by ELISA in vitreous samples were 0.11 ± 0.12 ng/mL in VRL, 0.002 ± 0.006 ng/mL in controls, and 0 ng/mL in ocular sarcoidosis. For YWHAG, the concentrations were 1.48 ± 0.75 ng/mL in VRL, 0.002 ± 0.005 ng/mL in controls, and 0.21 ± 0.60 ng/mL in ocular sarcoidosis. The vitreous levels of both PSAT1 and YWHAG were significantly higher in VRL (PSAT1: $P < 0.05$ vs. control and vs. ocular sarcoidosis; YWHAG: $P < 0.01$ vs. control and vs. ocular sarcoidosis) (Fig. 4). The vitreous concentrations of the 20S/26S proteasome complex were 13.7 ± 7.3 ng/mL in controls, 65.2 ± 44.4 ng/mL in ocular

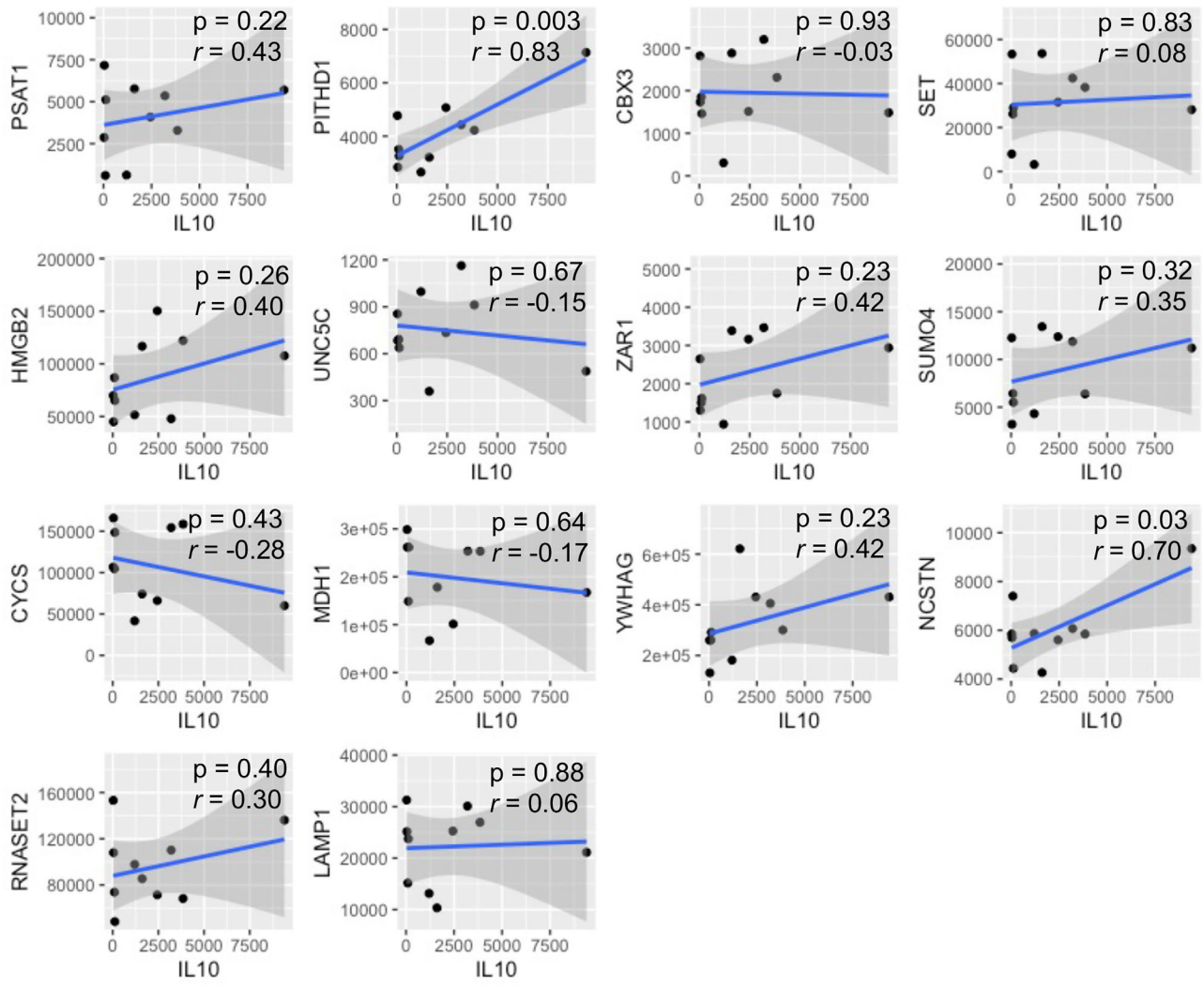

Figure 5. Correlation between DEPs and IL-10 in the vitreous of patients with vitreoretinal lymphoma. The relationship between IL-10 and nine DEPs that were upregulated in VRL compared with both controls and ocular sarcoidosis was analyzed using Pearson's correlation coefficient. A positive correlation was observed between IL-10 and both PITHD1 ($P = 0.003$) and NCSTN ($P = 0.03$).

sarcoidosis, and 363.8 ± 251.6 ng/mL in VRL, showing a significant stepwise increase in expression from control to ocular sarcoidosis and then to VRL ($P < 0.01$ for VRL vs. control and vs. ocular sarcoidosis, and for sarcoidosis vs. control). Therefore, the 14 proteins and proteasome pathways are potentially unique to VRL and may also prove crucial in understanding the pathogenesis of both VRL and ocular sarcoidosis.

Finally, we analyzed the association of IL-10 with the 14 DEPs that were upregulated in VRL compared with both controls and ocular sarcoidosis. A positive correlation was observed between IL-10 and PITHD1 ($P = 0.003$) and between IL-10 and NCSTN ($P = 0.03$) (Fig. 5). This finding suggests that these two proteins may have an impact on the pathogenesis of VRL.

Discussion

Proteomics is a promising bioinformatic approach that aims to improve diagnosis and elucidate the pathogenesis of diseases.[29] Numerous proteomic analyses of systemic lymphomas using serum and tissue samples have been reported.[15–17,30] These analyses have contributed to unravel the pathogenesis of lymphomas and hold promise for the development of specific biomarkers for malignant lymphomas.[31,32] Rüetschi et al.[16] conducted stable isotope labeling using amino acids in cell culture (SILAC)-based quantitative proteomic analysis of two distinct DLBCL patient groups with different clinical outcomes, and revealed that elevated protein expression of actin cytoskeleton protein network may be functionally associated with response to immunotherapy. Moreover, Zhang et al.[15] reported that proteomic patterns identified through comprehensive protein analysis using serum of patients with DLBCL achieved identification of patients with poor prognosis with 94% sensitivity. Therefore, protein expression patterns in patients with lymphomas are altered significantly depending on the stage of disease progression. These disparities may guide the development of novel treatment strategies for and enhance prognostic prediction of malignant lymphoma.

In the field of ophthalmology, comprehensive proteomic analyses of normal human vitreous[13,33] and vitreous of

patients with different uveitis etiologies[34,35] contribute to elucidation of the pathogenesis of ocular inflammation. Our group has also conducted proteomic analyses of various uveitis entities including experimental autoimmune uveoretinitis[36], Beçhet disease,[37] and ocular sarcoidosis.[14] However, to the best of our knowledge, comprehensive proteomic analysis of VRL using vitreous samples has not been reported due to the rarity of VRL. Therefore, the present results of comprehensive proteomic analysis derived from vitreous samples from patients with VRL are anticipated to contribute significantly to elucidation of the local pathophysiology associated with malignant lymphoma, a disease with poor prognosis.

In the proteomic analysis of patients with VRL compared with controls, 1163 proteins were found in controls, and 1571 were detected in patients with VRL. Additionally, of the 282 DEPs in VRL, 249 were upregulated. These findings imply that a substantial number of proteins are upregulated in the pathological conditions associated with VRL. Further, enrichment pathway analysis of these DEPs revealed substantial alterations within the proteasome pathway, suggesting that the ubiquitin proteasome system (UPS) may play a crucial role in the pathophysiology of VRL.

The UPS is a complex system in cells that controls the degradation of most proteins and regulates a variety of cellular processes.[38] This system plays a crucial role in various cellular functions, including cell cycle progression, signal transduction, and oxidative stress responses. Dysfunction of the UPS has been implicated in many diseases, including neurodegenerative diseases such as Parkinson disease and Alzheimer disease, autoimmune diseases, and neoplastic diseases such as malignant lymphoma.[39] Many B-cell lymphomas exhibit elevated expression of MYC oncoprotein, a transcription factor that upregulates many genes involved in proliferation and metabolism. MYC also promotes the expression of genes involved in the UPS, suggesting that upregulation of ubiquitination is a common feature of lymphoma.[40] The significance of mutated UPS genes in DLBCL is being investigated. Mutations of genes involved in UPS can affect protein degradation and signaling pathways that are important for lymphoma development. With this background, the regulation of UPS in malignant lymphomas is attracting attention as a novel therapeutic target. The association of ubiquitination with the pathogenesis of VRL has not been reported to date. Many ubiquitin enzymes are regulated by miRNAs, and reports have suggested that specific miRNAs such as miR-300 and miR-452 may regulate the ubiquitination of the target substrates in malignant tumors.[41,42] Interestingly, in our previous comprehensive miRNA sequence analysis of vitreous humor in VRL, we observed an increased expression of miR-452 in VRL.[10] To investigate the possible involvement of other miRNAs apart from miR-452, trans-omic analysis combining miRNA sequencing and proteomics is required in future studies. Inferring from previous findings related to ubiquitination in malignant lymphomas,[40,43] the present results may suggest that ubiquitin metabolism is altered in VRL as in systemic lymphomas.

Proteomic analysis identified 17 proteins as DEPs in VRL compared with ocular sarcoidosis, of which 16 were upregulated and one was downregulated. These results confirm that aberrantly expressed vitreous proteins in VRL are almost exclusively upregulated even when compared with a granulomatous uveitis. Fourteen DEPs with significantly elevated expression levels compared with both controls and ocular sarcoidosis were considered to be potential vitreous biomarkers for VRL. These proteins include a subset of proteasome 20S proteins, along with UPS-related proteins such as SUMO4. In particular, YWHAG, which is named 14-3-3 protein gamma, showed significantly increased expression in the vitreous compared with control and ocular sarcoidosis. The 14-3-3 family proteins consist of seven isoforms in mammals.[44] They are involved in diverse functions in cell proliferation and cancer progression, and their interaction with target proteins can alter their localization, stability, conformation, phosphorylation, and other properties.[45,46] The relationship between 14-3-3 proteins and lymphoma is complex and not fully understood; however, some studies have implicated 14-3-3 proteins in the pathogenesis of lymphoma and suggested that they may be potential targets for therapy. Li et al.[47] reported that low 14-3-3beta expression was associated with poor survival in DLBCL patients. In addition, Maxwell et al.[48] reported that 14-3-3zeta mediated resistance of DLBCL to chemotherapy and suggested a combination strategy with a 14-3-3 inhibitor for the treatment of DLBCL. These reports suggest that alterations in the expression patterns of the 14-3-3 family proteins could be closely involved in treatment response and prognosis of DLBCL.

In this study, PITHD1 and NCSTN proteins correlated positively with IL-10 in the vitreous. Proteasome interacting domain-containing protein 1 (PITHD1) is a protein-coding gene that plays various roles associated with cellular processes, and NCSTN is a subunit of a protein complex referred to as gamma-secretase that plays a critical role in cell signaling pathways. There are no reports suggesting a direct relationship of the role of IL-10 in both PITHD1 and NCSTN proteins. This may be attributed to the limited understanding of the mechanisms underlying IL-10 upregulation in lymphoid tumor cells of VRL. Therefore, our findings proposing an association of these proteins with VRL may provide insights into the understanding of pathophysiology of IL-10 elevation in VRL.

From the comprehensive proteomic analyses, three proteins with significantly elevated expression levels in VRL (PSAT, YWHAG, and the 20S/26S proteasome complex) emerged as candidate marker proteins. Validation of vitreous concentrations of these proteins measured by ELISA showed that all three were significantly higher in VRL than in controls and ocular sarcoidosis. Further investigations of these proteins as biomarkers of VRL are warranted.

This study has several limitations. Primarily, the research was conducted using retrospectively collected samples. As a result, the duration from disease onset to vitrectomy varies, which could mean that disease progression is not uniform across the samples. Moreover, prior to the proteomic analysis, sample handling conditions such as the interval between centrifugation and storage and the storage temperature were not strictly controlled, possibly leading to accelerated proteolysis. These issues necessitate further prospective studies to validate the present findings. Another limitation is the relatively small sample size due to the rarity of VRL, which limits the detection of statistical significance of the findings. Finally, as a single-center, case-control study, this research might incorporate sampling biases including geographic location, race, age, and gender. Despite the challenges associated with the rarity of VRL in conducting prospective cohort studies, including cost and time constraint, further research is warranted to validate the present findings by

Investigative Ophthalmology & Visual Science

increasing the number of patients with VRL and comparing with a carefully matched control group.

Conclusions

We present for the first time a comprehensive proteomic analysis of vitreous humor from patients with VRL. Our extensive protein analysis demonstrates that proteins expressed in the vitreous of patients with VRL were altered markedly when compared with patients with macular hole or epiretinal membrane and patients with ocular sarcoidosis. The DEPs identified in this study may play critical roles in the pathogenesis of VRL. These findings enhance our understanding of the pathogenesis of VRL and potentially contribute to the development of biomarkers.

Acknowledgments

The authors thank members of the Department of Ophthalmology, Tokyo Medical University Hospital, for their assistance in collecting clinical data, and Teresa Nakatani for editorial support.

Supported in part by Grants-in-Aid for Scientific Research (16K11304 and 19K09981) from the Ministry of Education, Culture, Sports, Science, and Technology of Japan.

Disclosure: **H. Komatsu**, None; **Y. Usui**, None; **K. Tsubota**, None; **R. Fujii**, None; **T. Yamaguchi**, None; **K. Maruyama**, None; **R. Wakita**, None; **M. Asakage**, None; **K. Hamada**, None; **N. Yamakawa**, None; **N. Nezu**, None; **K. Ueda**, None; **H. Goto**, None

References

1. Soussain C, Malaise D, Cassoux N. Primary vitreoretinal lymphoma: a diagnostic and management challenge. *Blood*. 2021;138(17):1519–1534.
2. Sagoo MS, Mehta H, Swampillai AJ, et al. Primary intraocular lymphoma. *Surv Ophthalmol*. 2014;59(5):503–516.
3. Sonoda K-H, Hasegawa E, Namba K, Okada AA, Ohguro N, Goto H. Epidemiology of uveitis in Japan: a 2016 retrospective nationwide survey. *Jpn J Ophthalmol*. 2021;65(2):184–190.
4. Kimura K, Usui Y, Goto H. Clinical features and diagnostic significance of the intraocular fluid of 217 patients with intraocular lymphoma. *Jpn J Ophthalmol*. 2012;56(4):383–389.
5. Kim MM, Dabaja BS, Medeiros J, et al. Survival outcomes of primary intraocular lymphoma: a single-institution experience. *Am J Clin Oncol*. 2016;39(2):109–113.
6. Chan CC, Sen HN. Current concepts in diagnosing and managing primary vitreoretinal (intraocular) lymphoma. *Discov Med*. 2013;15(81):93–100.
7. Kunimi K, Usui Y, Sugawara R, et al. Clinical features of primary vitreoretinal lymphoma developing extra-central nervous system (CNS)/testicular lymphomas with or without CNS involvement: a single-centre study of 13 case. *Br J Haematol*. 2023;201(1):158–161.
8. Davis JL. Diagnosis of intraocular lymphoma. *Ocul Immunol Inflamm*. 2004;12(1):7–16.
9. Sen HN, Bodaghi B, Hoang PL, Nussenblatt R. Primary intraocular lymphoma: diagnosis and differential diagnosis. *Ocul Immunol Inflamm*. 2009;17(3):133–141.
10. Minezaki T, Usui Y, Asakage M, et al. High-throughput microRNA Profiling of vitreoretinal lymphoma: vitreous and serum microRNA profiles distinct from uveitis. *J Clin Med*. 2020;9(6):1844.
11. Chowdhury UR, Madden BJ, Charlesworth MC, Fautsch MP. Proteome analysis of human aqueous humor. *Invest Ophthalmol Vis Sci*. 2010;51(10):4921.
12. Smith JR, David LL, Appukuttan B, Wilmarth PA. Angiogenic and immunologic proteins identified by deep proteomic profiling of human retinal and choroidal vascular endothelial cells: potential targets for new biologic drugs. *Am J Ophthalmol*. 2018;193:197–229.
13. Murthy KR, Goel R, Subbannayya Y, et al. Proteomic analysis of human vitreous humor. *Clin Proteomics*. 2014;11(1):29.
14. Komatsu H, Usui Y, Tsubota K, et al. Comprehensive proteomic profiling of vitreous humor in ocular sarcoidosis compared with other vitreoretinal diseases. *J Clin Med*. 2022;11(13):3606.
15. Zhang X, Wang B, Zhang X-S, Li Z-M, Guan Z-Z, Jiang W-Q. Serum diagnosis of diffuse large B-cell lymphomas and further identification of response to therapy using SELDI-TOF-MS and tree analysis patterning. *BMC Cancer*. 2007;7(1):235.
16. Rüetschi U, Stenson M, Hasselblom S, et al. SILAC-based quantitative proteomic analysis of diffuse large B-cell lymphoma patients. *Int J Proteomics*. 2015;2015:841769.
17. Schröder C, Srinivasan H, Sill M, et al. Plasma protein analysis of patients with different B-cell lymphomas using high-content antibody microarrays. *Proteomics Clin Appl*. 2013;7(11-12):802–812.
18. Mörth C, Sabaa AA, Freyhult E, et al. Plasma proteome profiling of cardiotoxicity in patients with diffuse large B-cell lymphoma. *Cardiooncology*. 2021;7(1):6.
19. Whitcup SM, Stark-Vancs V, Wittes RE, et al. Association of interleukin 10 in the vitreous and cerebrospinal fluid and primary central nervous system lymphoma. *Arch Ophthalmol*. 1997;115(9):1157–1160.
20. Coupland SE, Bechrakis NE, Anastassiou G, et al. Evaluation of vitrectomy specimens and chorioretinal biopsies in the diagnosis of primary intraocular lymphoma in patients with masquerade syndrome. *Graefes Arch Clin Exp Ophthalmol*. 2003;241(10):860–870.
21. Usui Y, Wakabayashi Y, Okunuki Y, et al. Immune mediators in vitreous fluids from patients with vitreoretinal B-Cell lymphoma. *Invest Ophthalmol Vis Sci*. 2012;53(9):5395.
22. Nezu N, Usui Y, Saito A, et al. Machine learning approach for intraocular disease prediction based on aqueous humor immune mediator profiles. *Ophthalmology*. 2021;128(8):1197–1208.
23. Okuda S, Watanabe Y, Moriya Y, et al. jPOSTrepo: an international standard data repository for proteomes. *Nucleic Acids Res*. 2017;45(D1):D1107–D1111.
24. Ikeda A, Nagayama S, Sumazaki M, et al. Colorectal cancer-derived CAT1-positive extracellular vesicles alter nitric oxide metabolism in endothelial cells and promote angiogenesis. *Mol Cancer Res*. 2021;19(5):834–846.
25. Gillespie M, Jassal B, Stephan R, et al. The reactome pathway knowledgebase 2022. *Nucleic Acids Res*. 2022;50(D1):D687–D692.
26. Ge SX, Jung D, Yao R. ShinyGO: a graphical gene-set enrichment tool for animals and plants. *Bioinformatics*. 2020;36(8):2628–2629.
27. Zhou Y, Zhou B, Pache L, et al. Metascape provides a biologist-oriented resource for the analysis of systems-level datasets. *Nat Commun*. 2019;10(1):1523.
28. Benjamini Y, Hochberg Y. Controlling the false discovery rate: a practical and powerful approach to multiple testing. *J R Stat Soc Series B Stat Methodol*. 1995;57(1):289–300.
29. Adhikari S, Nice EC, Deutsch EW, et al. A high-stringency blueprint of the human proteome. *Nat Commun*. 2020;11(1):5301.

Investigative Ophthalmology & Visual Science

30. Xu W, Hu Y, He X, et al. Serum profiling by mass spectrometry combined with bioinformatics for the biomarkers discovery in diffuse large B-cell lymphoma. *Tumour Biol*. 2015;36(3):2193–2199.
31. Ding Z, Wang N, Ji N, Chen Z-S. Proteomics technologies for cancer liquid biopsies. *Mol Cancer*. 2022;21(1):53.
32. Romesser PB, Perlman DH, Faller DV, Costello CE, McComb ME, Denis GV. Development of a malignancy-associated proteomic signature for diffuse large B-cell lymphoma. *Am J Pathol*. 2009;175(1):25–35.
33. Aretz S, Krohne TU, Kammerer K, et al. In-depth mass spectrometric mapping of the human vitreous proteome. *Proteome Sci*. 2013;11(1):22.
34. Kasudhan KS, Sarkar S, Gupta V, Gupta A, Chakraborti A. Identification of unique proteins in vitreous fluid of patients with noninfectious uveitis. *Acta Ophthalmol*. 2018;96(8):e989–e1003.
35. Schrijver B, Kolijn PM, Berge JCEM, et al. Vitreous proteomics, a gateway to improved understanding and stratification of diverse uveitis aetiologies. *Acta Ophthalmol*. 2022;100(4):403–413.
36. Okunuki Y, Usui Y, Kezuka T, et al. Proteomic surveillance of retinal autoantigens in endogenous uveitis: implication of esterase D and brain-type creatine kinase as novel autoantigens. *Mol Vis*. 2008;14:1094–1104.
37. Okunuki Y, Usui Y, Takeuchi M, et al. Proteomic surveillance of autoimmunity in Behcet's disease with uveitis: selenium binding protein is a novel autoantigen in Behcet's disease. *Exp Eye Res*. 2007;84(5):823–831.
38. Ciechanover A, Schwartz AL. The ubiquitin-proteasome pathway: the complexity and myriad functions of proteins death. *Proc Natl Acad Sci USA*. 1998;95(6):2727–2730.
39. Gong B, Radulovic M, Figueiredo-Pereira ME, Cardozo C. The ubiquitin-proteasome system: potential therapeutic targets for Alzheimer's disease and spinal cord injury. *Front Mol Neurosci*. 2016;9:4.
40. Best S, Hashiguchi T, Kittai A, et al. Targeting ubiquitin-activating enzyme induces ER stress-mediated apoptosis in B-cell lymphoma cells. *Blood Adv*. 2019;3(1):51–62.
41. Chen Z, Zhang W, Jiang K, et al. MicroRNA-300 regulates the ubiquitination of PTEN through the $CRL4B^{DCAF13}$ E3 ligase in osteosarcoma cells. *Mol Ther Nucleic Acids*. 2018;10:254–268.
42. Goto Y, Kojima S, Kurozumi A, et al. Regulation of E3 ubiquitin ligase-1 (WWP1) by microRNA-452 inhibits cancer cell migration and invasion in prostate cancer. *Br J Cancer*. 2016;114(10):1135–1144.
43. Di Costanzo A, Del Gaudio N, Conte L, Altucci L. The ubiquitin proteasome system in hematological malignancies: new insight into its functional role and therapeutic options. *Cancers*. 2020;12(7):1898.
44. Fu H, Subramanian RR, Masters SC. 14-3-3 Proteins: structure, function, and regulation. *Annu Rev Pharmacol Toxicol*. 2000;40:617–647.
45. Freeman AK, Morrison DK. 14-3-3 Proteins: diverse functions in cell proliferation and cancer progression. *Semin Cell Dev Biol*. 2011;22(7):681–687.
46. Morrison DK. The 14-3-3 proteins: integrators of diverse signaling cues that impact cell fate and cancer development. *Trends Cell Biol*. 2009;19(1):16–23.
47. Li C, Li Z, Zhang M. Low expression of 14-3-3beta is associated with adverse survival of diffuse large B-cell lymphoma patients. *Front Med (Lausanne)*. 2019;6:237.
48. Maxwell SA, Li Z, Jaya D, Ballard S, Ferrell J, Fu H. 14-3-3ζ mediates resistance of diffuse large B cell lymphoma to an anthracycline-based chemotherapeutic regimen. *J Biol Chem*. 2009;284(33):22379–22389.

Investigative Ophthalmology & Visual Science